Molecular Crystals and Liquid Crystals Science and Technology. Section A. Molecular Crystals and Liquid Crystals

Publication details, including instructions for authors and subscription information:
http://www.tandfonline.com/loi/gmcl19

Studies on Addressing Techniques for Bistable Ferroelectric Liquid Crystal Cells

Paolo Maltese [a] , Vincenzo Ferrara [a] & Angelo Coccettini [a]

[a] Department of Electronic Engineering, La Sapienza University, Via Eudossiana 18, 00184, Roma, Italy

Version of record first published: 23 Sep 2006.

To cite this article: Paolo Maltese , Vincenzo Ferrara & Angelo Coccettini (1995): Studies on Addressing Techniques for Bistable Ferroelectric Liquid Crystal Cells, Molecular Crystals and Liquid Crystals Science and Technology. Section A. Molecular Crystals and Liquid Crystals, 266:1, 163-177

To link to this article: http://dx.doi.org/10.1080/10587259508033640

Mol. Cryst. Liq. Cryst. 1995, Vol. 266, pp. 163–177
Reprints available directly from the publisher
Photocopying permitted by license only

STUDIES ON ADDRESSING TECHNIQUES FOR BISTABLE FERROELECTRIC LIQUID CRYSTAL CELLS

PAOLO MALTESE, VINCENZO FERRARA, ANGELO COCCETTINI
Department of Electronic Engineering, La Sapienza University,
Via Eudossiana 18, 00184 Roma (Italy)

Abstract A classification of all the known addressing modes is proposed and related to our simple uniform director model for the addressed FLC cell. Two addressing tricks are explained which have been found by extensive simulations with the model. Addressing experiments with our modes at 12 μs line addressing time are presented. Computer-plotted voltage-time regions of operations for several addressing modes are discussed.

INTRODUCTION

The art of addressing a matrix display panel composed of bistable cells, arranged in M rows by N columns, consists of repeated steps in which the states latched by the M pixels in a particular row are controlled in as short as possible time-windows, without affecting the pixels in the other rows. This results from the combined application of a data independent selection waveform on the row, and of data waveforms on the M columns. The entire NxM panel can be written in N consecutive control windows, whose duration is known as line addressing time. The internal memory makes the contrast independent from N, if N is large. With FLC cells, the short line-addressing times available are compatible with the information content and refreshing rate requested for TV displays. Whereas using the standard nematic cells, without electronic switches incorporated into each cell, the optical contrast is severely reduced for large values of N (N>50).

A large variety of bistable FLC matrix-addressing techniques has been presented since 1985[1,2] and new ones are still being developed. The studies have been slowed down by poor understanding of the addressing effects and by the persisting inavailability of integrated circuit drivers suitable to implement the most advanced addressing techniques. Actual understanding dates back to the proposal by P. Maltese of a dynamic model in 1991[3]. The main addressing properties of the cells have been defined through it[4] and their high speed addressing limits[5,6,7] have been related to the biaxial properties of the dielectric tensor of the liquid crystal.

Aim of this paper is to discuss the operating principles of the known addressing modes and to propose a new classification for them. To do this, the addressing model is preliminarly presented as a reference. Improvements in addressing from two recently introduced compensation techniques will also be reported, along with detailed experimental waveforms. Moreover, in order to compare different addressing modes, we present their voltage-time regions of existence as computed from the model for a typical simulation cell.

AN ADDRESSING EFFECTIVE MODEL

To take into account in the simplest way the effects deriving from the chevron structure of the smectic layers[8], tilted layers are assumed, so obtaining a simpler structure which can be equivalent when viewed from the normal direction. Though crude, uniform director models have been generally used to model the optical switching of the SSFLC cell. A simple addressing effective dynamic equation using a single state variable has been obtained[3,4] by considering the dielectric, polarization and viscosity torques acting on a uniform director and by adding the simplest possible heuristic expression for the elastic torque, whose importance is only secondary when large voltages are used to obtain fast addressing.

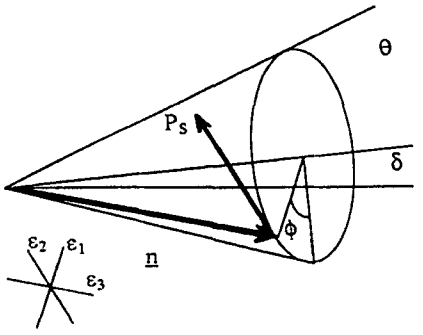

Figure 1 - In the SmC* phase, the director **n** makes the characteristic angle θ to the normal to the smectic layers, tilted at an angle δ. The spontaneous polarization $\mathbf{P_s}$ is orthogonal to **n**, lies in the plane of the layers and is tangential to the circle. The rotation of **n** on the surface of the cone by an angle ϕ implies a rotation of the projection in the plane of the cell of the optical axis. The biaxial dielectric tensor is characterized by the three constants ε_1, ε_2 (along $\mathbf{P_s}$) and ε_3 (along **n**). $\Delta\varepsilon = \varepsilon_3 - \varepsilon_1$ and $\partial\varepsilon = \varepsilon_2 - \varepsilon_1$ are respectively the relative dielectric anisotropy and biaxiality. $\varepsilon_\Delta = \partial\varepsilon - \Delta\varepsilon \sin^2\theta$ is the effective relative dielectric biaxiality.

As shown in Figure 1, the liquid crystal director **n** lies along the surface of a cone defining an angle $\theta \approx 15 \div 45°$ to the perpendicular of the smectic layers. When the cell walls are horizontal the smectic layers are tilted from the vertical (and the cone axis from the horizontal) by an angle $\delta = 0.8\theta \div 0.9\theta$. In special cases smaller or even zero values can be obtained for δ, corresponding to quasi-bookshelf or ideal bookshelf structures. The director can be switched between two approximately horizontal surface-stabilized positions by pulsed fields interacting with the spontaneous polarization of the liquid crystal (P_s= 1÷100 nC/cm^2). The optical behaviour is approximately the same of a birefringent slab, whose axis can rotate in the cell's plane through an angle $<2\theta$. Crossed polarizers can extinguish the light in one state and transmit light in the other state.

The angle $\phi(t)$ of the director around the cone, also defined in Figure 1, identifies the state of the cell and, in the usual cases, has a one to one correspondence with its optical transmission. From the equilibrium of torques, the rate of change of ϕ, in terms of a reduced time $t'=t/2T_c$, can be related to a reduced voltage $V'=V/V_c$ as [3]:

$$\frac{d\phi}{dt'} = V' \cos\phi \left[1 + (\sin\phi - \cos\phi_0 \tan\phi)\frac{1}{V'\sqrt{\lambda}} + (\sin\phi - \cos\phi_V \tan\phi)\frac{V'}{\sqrt{\lambda}} \right] \qquad (1)$$

normalized by defining, for the cell, a real positive characteristic voltage V_c, a characteristic time T_c , the stable angles ϕ_0 , for no voltage applied, and ϕ_V , for infinite voltage, and a "voltage linearity range" λ .

This simple phenomenologic equation is able to explain the occurrence of a minimum pulse duration for latching with monopolar pulses, to reproduce both trailing and leading pulse latching as well as to describe complex addressing phenomena in terms of simple liquid crystal and cell properties[4].

As can be seen from equation (1), $V_c/\sqrt{\lambda}$ and $V_c\sqrt{\lambda}$ represent the approximate limits for V between which both the elastic and dielectric torques can be considered smaller than the polarization torque. In a logarithmic voltage scale, λ measures the width of the voltage range, centered around V_c, inside which the switching time is inversely proportional to the applied voltage. The relative magnitude of the other torques with respect to the ferroelectric torque has a minimum of the order of $1/\sqrt{\lambda}$ when $V \cong V_c$. Even if they are small the existence of such torques is essential to provide matrix-addressing capabilities to the cell[4]. Unfortunately they had never been measured before the present efforts in our laboratory[9].

In physical terms, the relevant parameters can be expressed as:

$$V_c = \frac{d}{\cos\delta}\sqrt{\frac{2\eta_c}{\varepsilon_o\varepsilon_\Delta T_r}} \quad ; \quad T_c = \frac{\sqrt{\varepsilon_o\varepsilon_\Delta T_r \eta_c / 2}}{P_s} \tag{2}$$

$$\lambda = \frac{P_s^2 T_r}{2\varepsilon_o\varepsilon_\Delta\eta_c} = \left(\frac{T_r}{2T_c}\right)^2 \quad ; \quad \cos\phi_v = -\frac{\Delta\varepsilon \sin 2\theta \tan\delta}{2\varepsilon_\Delta} \tag{3}$$

in which ε_0 is the vacuum dielectric constant, d is the cell thickness and T_r is an observable relaxation time constant, introduced here in its ratio with the rotational viscosity of the **n**-projection onto the smectic planes (an independently observable quantity) η_c, to describe the overall effective elastic behaviour of the cell.

The magnitude of V_c is related to the hf stabilization effects in the cell. In fact, if only a very high frequency voltage is applied, with rms amplitude V_{hf} and zero mean value, the equilibrium angle around which ϕ oscillates is given by:

$$\cos\phi = \frac{V_c^2\cos\phi_0 + V_{hf}^2\cos\phi_v}{V_c^2 + V_{hf}^2} \tag{4}$$

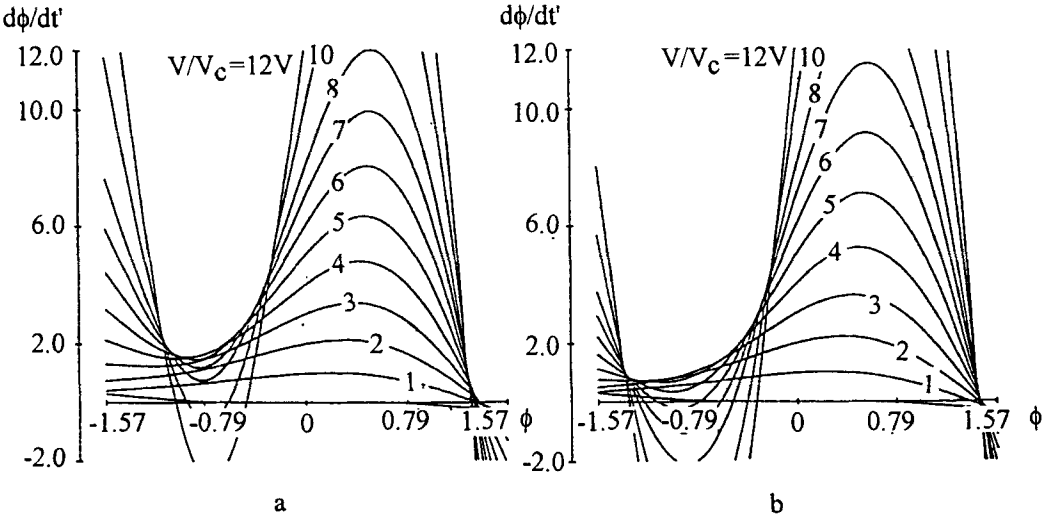

Figure 2 - Plots of $d\phi/dt'$ as a function of ϕ for different values of V' corresponding to the differential equation (1), to which the addressing behaviour of the SSFLC cell is reduced. Both plots are for ϕ_0=0.4 rad and λ=10; a) is the plot for our typical simulation cell, in which ϕ_V=1.2 rad, and b) is for ϕ_V=1.4 rad.

Two examples of plot of the right-hand term in equation (1), in the region of our interest for ϕ, and for large positive reduced voltages V', are shown in Figure 2. Figure 2a corresponds to our standard simulation chevron cell, Figure 2b to a case in better physical agreement with some commercial Merck material, such as ZLI5014. The curves are symmetric for negative voltages in the sense that the rates of change are the opposite to those for opposite values of ϕ, shown in the figure. For different values of the parameters, the general shape of the curves remains the same. The curves for V'=0 correspond to an elastic torque only. The reduced rate of change of ϕ is always positive in the range $-\phi_V < \phi < +\phi_V$, above a small and below a large value of V' between which square-wave switching from one extreme state to the other is possible.

BASIC ADDRESSING MECHANISMS

Before introducing three basic mechanisms according to which all known bistable FLC addressing techniques can be classed, it will be useful to recall our introduction and complete its definitions.

In a line-at-time direct addressing technique, as those here concerned, each pixel in the same row (or line) is simultaneously driven into a state depending only on the (data or column) voltage waveform present on the column corresponding to the pixel in a particular time segment or "control window". Such (usually consecutive) time windows define a selection or scanning cycle of the matrix. The voltage waveforms applied on the rows are indipendent on the displayed image but each of them determines a corresponding control time window, so that we can term them "selection voltages". For nematic addressing the selection waveforms are just selection pulses and the control windows are defined by their widths.

On the contrary, in bistable FLC addressing, selection sequences longer than the corresponding control windows can be used [5,6]. They can be composed by several pulses which can be termed in accordance with their effect on the state of the cell [5,6], detectable by its time varying light transmission between crossed polarizers, shortly termed response of the cell.

"Erasing" or "blanking" pulses at the begining of the selection sequence can produce the same response at their end for any initial state of the cell and for any data voltage, intended for the control of the state of pixels on other rows, simultaneously applied on the column electrode of the cell. On the contrary, we term "writing" pulse the pulse near the end of the selection sequence, for which the response at its end can be different enough, according to the data waveform in the control window, to latch

the cell into different final states.

All known addressing modes make use, in the data waveforms, of dc balanced segments in each control window. This condition is requested by the magnitude of the ferroelectric torques in the cell, usually much larger than the elastic and dielectric ones. If this is true, to a first approximation the cell state has a one to one correspondence with $\int_{t_o}^{t} V(t)dt$. If a dc component were present in each segment of a data waveform, after many segments the voltage integral could reach values high enough to switch the cell into the other state, even in the absence of selection voltage. The presence of data-dependent segments addressing all the pixels in the same column would result in long-term bistability being destroyed for displayed patterns originating long sequences of equal data. This is always considered true in the practical cases.

However, in the same approximation, no effect would result from the superposition of any dc-balanced data voltage with any selection voltage waveform, so that matrix addressing would be impossible.

A condition for FLC cell addressing was first proposed by Lagerwall et al. in 1985[1], according to which a state change occurs in a cell when a pulse in the voltage across it exceeds a critical pulse area. This explanation can still be used for the earlier classical addressing modes. Later they have been termed "normal" or "low voltage" modes, in contrast to "high voltage" modes[6,10,11].

The addressing model presented in the former section allows a better understanding for the "low voltage" modes but it is not necessary for a simple explanation of their operation. On the contrary, we will make use of the simplest formal addressing model able to predict "low voltage" addressing by means of the concept of critical pulse area, propo-sed by Maltese in 1992[11]. This model corresponds to take into account only the ferroelectric torques (as for $\lambda = \infty$ in eq. (1), with finite V_C and T_C and $\varepsilon_\Delta = 0$, $T_r = \infty$) and to arbitrarily introduce positive and negative saturations in the response (otherwise addressing would be impossible[4]). A voltage pulse of arbitrary shape and polarity, applied at times t1 to t2, drives the cell from one saturated response to the other when $\left|\int_{t_1}^{t_2} V(t)dt\right| \geq 2A_c$, where A_c is a critical pulse area.

Once more we define a first class of "low voltage" addresing modes with reference to the modes expected in this model. Their essential feature is the saturation in the response to the driving voltage at the end of a first pulse before a writing pulse in the selection waveform. The latter is usually (but not necessarily) the last pulse in the

selection sequence and its area is modified by the last part of the data voltage in the control window so that the resulting area of the writing pulse controls the state latched in the cell. The sketch in Figure 3 summarizes this definition. Other pulses, for deeper erasing or dc compensation, may precede the first pulse shown. This class includes: the Seiko Instuments[2] and the Toshiba[12] addressing modes, for which the duration of the first pulse equals the duration of the writing pulse; the 2-slot LETI-Bari[5,6] and GEC[13] modes, using a first pulse larger than the writing pulse; and the Hoechst overlapped modes[14], using a last pulse in each data segment shorter than the write pulse.

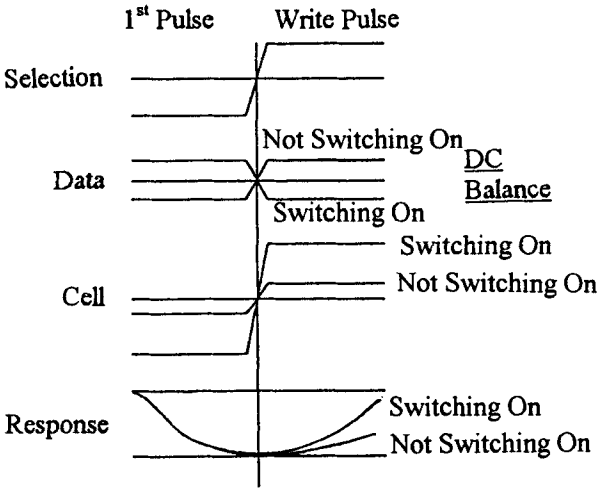

Figure 3 - Essential features of "low voltage" FLC addressing. The "Selection" voltage waveform on the row, the "Data" wavevorm on the column, the resulting waveform across the "Cell" and the optical "Response" are sketched. The area of the resulting writing pulse in the cell voltage controls the final state of the addressed pixel.

Very different techniques have been proposed for "high voltage" addressing, their common feature being the capability to exploit high voltage phenomena attributed to dielectric torques. They can be better understood with reference to the addressing model in the preceding section and to curves like those in Figure 2, whose experimental study is presently under way [9].

With reference to Figure 2a, square-wave switching becomes impossible above $V' \cong 9$. However, for negative angles, corresponding to the beginning of the switching process, the rate of change starts to decrease when $V' \cong 5$. The asymmetry between the left and right hand side of the curves is relevant at even lower reduced voltages and it is the same existing between curves for opposite applied voltages. The existence of high-voltage addressing modes is based on it and it is possible only for high enough

resulting voltages, corresponding to large enough asymmetries. In the model, to exploit these asymmetries at best, a control time window should be used in which ϕ oscillates about one or to the other of the values $\pm\pi/4$, to which approximately the largest dielectric torques correspond. Dc-balanced bipolar data featuring in the control window the same changes in sign existing in the selection voltage should be applied. Hence two basic "high voltage" addressing mechanisms exist, which can be termed "stopped writing" and "hampered writing". The former exploits the asymmetry in the curves on the side of the state reached at the end of the writing pulse (in proximity to $\pi/4$) and corresponds to the "Fast" and "Superfast" addres-sing modes that make use of stop pulses[6,15]. The latter exploits the same asymmetry in proximity of the initial state (and of $-\pi/4$) and corresponds to the Monopolar Pulse[10] and Malvern[16] Vt_{min} modes as well as to the new SDS mode in Figure 8.

The three basic mechanisms presented originate three classes of corresponding addressing modes. However intersections can exists in correspondence to modes in which more than one mechanism is present.

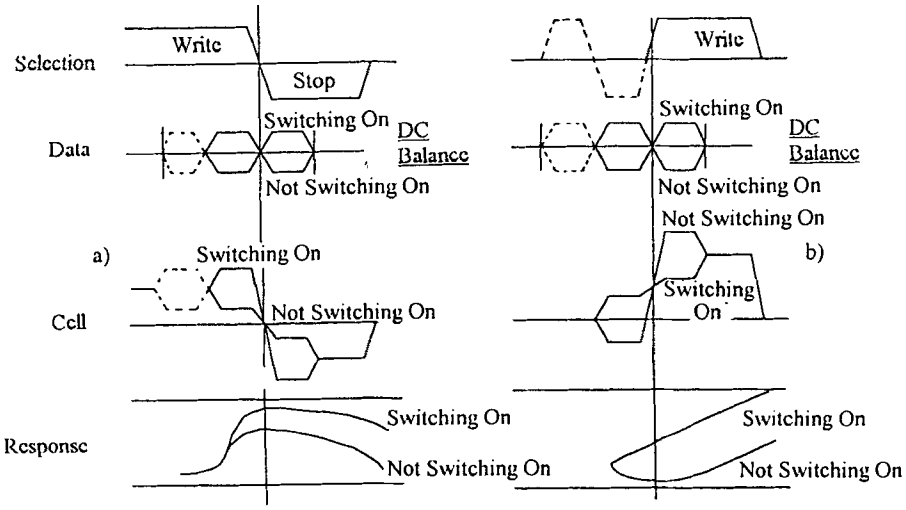

Figure 4 - Essential features of "high voltage" FLC addressing. The final state of the addressed pixel is controlled by the amplitude of hf components: a) at the end of the writing pulse (stopped writing modes); b) at the beginning of the writing pulse (hampered writing modes). Selection, Data, Cell and Response as in Figure 3.

COMPENSATION TECHNIQUES

The choice of addressing waveforms providing large enough effects of the data in the control window is not sufficient in itself. A second requirement is that of negligible effects from the other data segments. As discussed in the former section, this reason determines the need of dc balanced data segments. However unwanted effects are still present which can be virtually eliminated [15] by the use of data waveforms in each segment having also a zero first order momentum. Such waveforms correspond to an integral function having a zero average value and have been termed crosstalk-compensated data[6].

As shown in Figure 5 they null the average change in the light trasmission and in the state of the cell. Otherwise the restoring and dielectric torques during a serie of equal data can alter significantly, the initial state. When selection follows, the addressing effect must be larger than the effect from the spread in the initial state. The crosstalk-compensated data are more effective in the high voltage modes and mixed modes.

A final requirement for the addressing waveforms is their tolerance with respect to cell non uniformities, and variations in the operating conditions.

The fundamental dependence from equations (2) of the characteristic switching area (given by the product $V_C T_C$) on $\eta_c d / P_s$ and the temperature dependence of the viscosity determine large effects of thickness and temperature variations, similar to those corresponding to changes in the scales of voltages and times in the addressing waveforms.

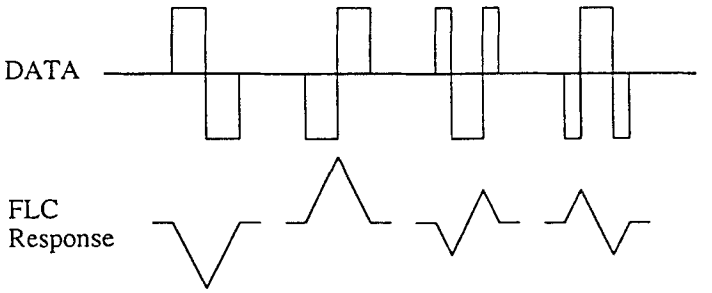

Figure 5 - Unlike the usually employed data on the left, the crosstalk compensated data on the right don't affect the average state of the cell during their application.

An addressing mode can be made tolerant to variations in the characteristic switching area if suitable compensation techniques are employed in the selection

waveforms, such that the different initial state of the cell compensates the different effect of the writing pulse. To obtain this behaviour one or more compensation pulses of suitable area can be used in the selection waveform just before the writing pulse, as in the example sketched in Figure 6. With no data applied, the final state of the cell is the same for different liquid crystal switching areas. Again this principle can be combined with different addressing techniques and remarkable results have been obtained together with Superfast addressing[17].

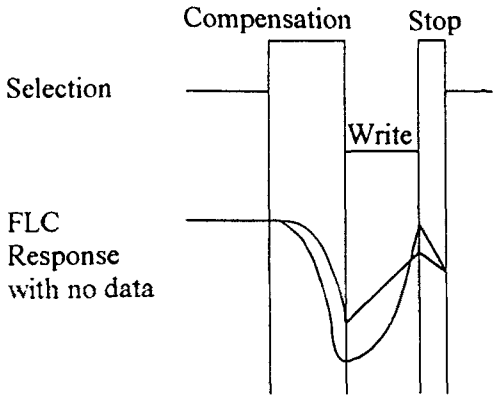

Figure 6 - Selection waveform providing compensation of variations in the characteristic switching area of the cell.

12 MICROSECOND ADDRESSING EXPERIMENTS

As an example, here we present the detailed experimental waveforms corresponding to some advanced addressing techniques recently reported by Maltese[17] for a ZLI4655/000 cell at 40 °C.

The left-hand part of Figure 7 illustrates a "high voltage" "Pause-Superfast" addressing mode (PS3) making use of crosstalk compensated data (and opposite polarities with respect to Figure 4a). To show the response in correspondence to the control window, the same expanded time scale of 10 μs/div is used for the traces a), b) and c). They represent the selection voltage, switching On and switching Off data voltages differing in the control window only and the corresponding two cases for the optical transmission respectively. Trace a) represents the write pulse and the stop pulse which overlap 2.75 and 1.25 data segments (control segments intended for other rows) respectively. At 200 μs/div, the same waveforms originate the traces d), for the selection voltage, and e), for the optical transmission. Only a small part of the frame

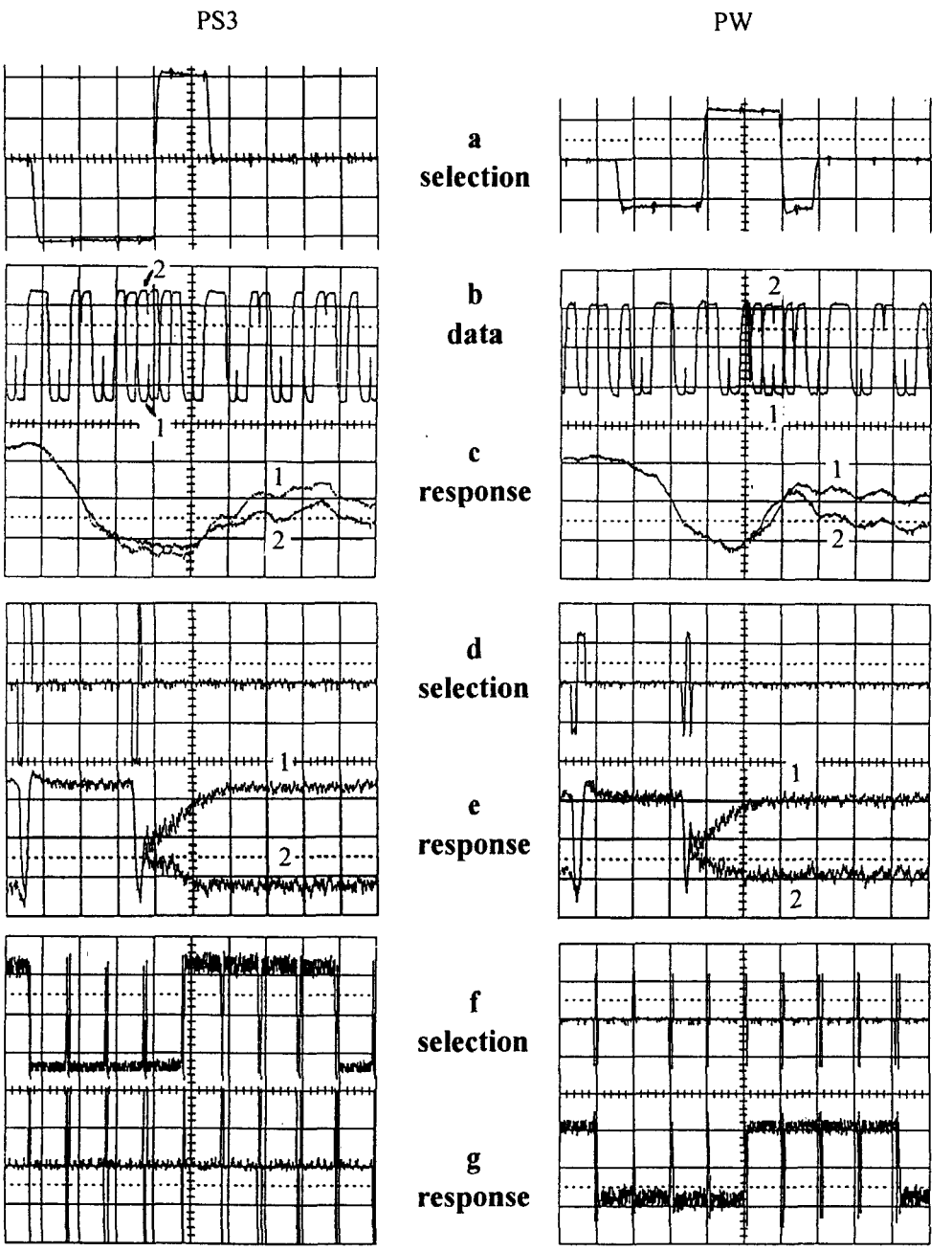

Figure 7 - Detailed waveforms for "Pause-Superfast" addressing (PS3, at left) and "Pause-Wide" addressing (PW, at right), for a ZLI4655/000 cell at 40°C and 12 μs line addressing time. Horizontal scales: a), b) and c) 10μs/div; d) and e) 200 μs/div; f) and g) 10 ms/div. Vertical scales: a), b) d) and f) 20 V/div; c), e) and g) arbitrary units (inverted).

period is still shown, corresponding to a dc balanced selection waveform starting with a double erase pulse and a pause, during which the cell is always in a dark state (corresponding to the higher level in the traces). The same waveforms are again shown at 10 ms/div (traces f) and g)), in correspondence to data switching the cell alternatively 4 frames on and 4 frames off.

With the same time and voltage scales, the right-hand part of Figure 7 illustrates a "high voltage" "Pause Wide Superfast" addressing mode (PW). As in Figure 6 but with opposite polarities. This mode also incorporates a pulse providing compensation against variations of the pulse switching area of the cell, visible in trace a) before the writing pulse and the stop pulse. Their lengths are respectively 2, 1.75 and 0.75 data segments. Here again dc balance is provided by a double erase pulse before a pause, visible in trace d).

At the expense of more complex selection waveforms, the experimental PW mode features two important advantages with respect to PS3: not only wider conditions of operation are obtained but also much smaller voltages can be used.

REGIONS OF OPERATION

In order to effectively compare the utility of different addressing modes, we map their regions of operation in a peak voltage - line addressing time bilogarithmic plane. From the preceding discussion it follows that the effect of temperature and thickness variations is similar to that of changes in the voltage and time scales. Hence an addressing technique tolerant to the former variations also corresponds to a large extension of its region of operation in the plane. From the addressing model, we have been able to computer-trace such regions for several addressing modes and for a range of simulation cells.

Figure 8a schematically shows several selection waveforms, each corresponding to an addressing mode, all making use for the data in their respective control windows of the same dc balanced bipolar pulses at the top of the Figure. In the reality different widths of the control window and different time scales correspond to the different modes. Figure 8b shows in the same way four addressing modes making use of crosstalk compensated data. N21 and HOE are "low voltage" modes. F431 is a "stopped writing" mode wich can also operate as a "low voltage mode" for smaller data amplitudes. PS2, PS3 and PW1/1' are "stopped writing" modes. MONO, MALV2, MALV3 and SDS are "hampered writing" modes. Our new "Stay Down pulse Superfast" mode[19] has been devised to improve the performance of the Malvern

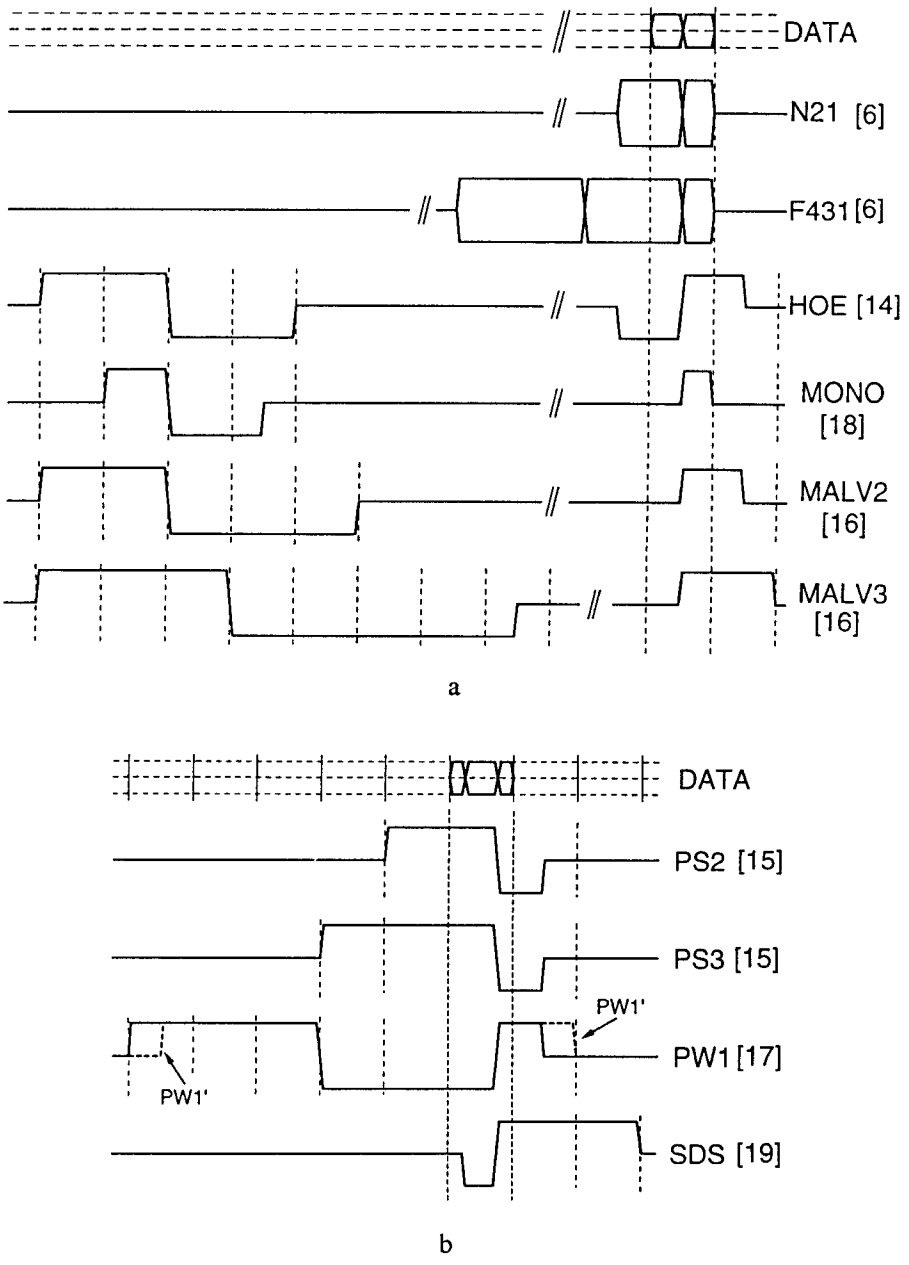

Figure 8 - Sketch of the waveforms used in different addressing modes (references in the Figure): a) making use of dc balanced bipolar pulses for the data; b) making use of crosstalk-compensated data and preceding double erase pulses not shown.

modes and to allow smaller selection voltages, by a more efficient use of the "hampered writing" mechanism, allowing also the use of crosstalk-compensated data.

The corresponding regions of operation, for our standard simulation cell, are plotted in Figure 9.

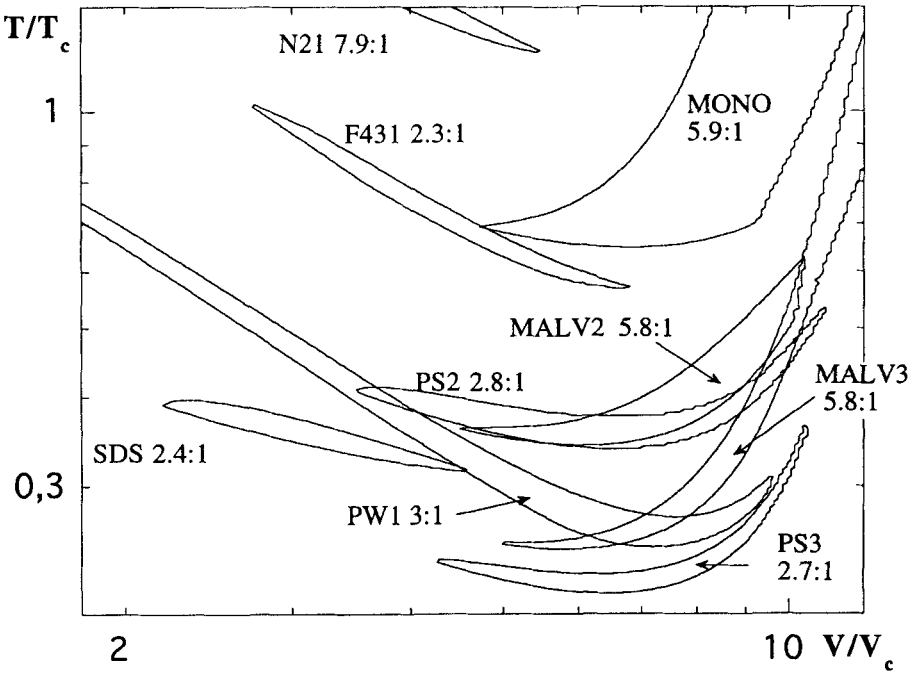

Figure 9 - Computed map of the regions of operation under worst case investigation for different addressing modes and our standard cell. Reduced line addressing times versus reduced total peak voltages. The ratios are indicated between selection and data peak voltages.

CONCLUSIONS

With the aid of simple models for addressing, we have been able to identify and discuss three basic addressing mechanisms, i. e. writing after a saturation, stopped writing and hampered writing, which can be used to class all addressing modes so far reported. We have also shown why and how two compensation techniques can be incorporated in the design of addressing modes and presented detailed experimental waveforms for the corresponding operation of real cells, at 12 μs line-addressing time. Finally we have presented the features of several addressing modes and we have computed their regions of operation in a standard cell to allow their comparison.

In general, both classes of high voltage modes are much faster than low voltage addressing. Without compensation techniques, hampered writing tends to produce wider regions of operation than stopped writing but it requires higher voltages. We are now introducing our compensation techniques and more complex selection waveforms in the hampered writing modes, with excellent results. For example, with SDS, the same cell as for Figure 7, operates at 12 μs line-addressing-time, with the use of only 16 V for the selection and 22 V for the data. In agreement with the simulation, lower voltages than those for PW (25 and 23 V) and PS3 (42 and 28 V) are required.

REFERENCES

[1] Lagerwall, S. T., Wahl, J., and Clark, N. A., *Conf. Record of the 1985 Intl. Display Research Conf.*, San Diego, Oct. 1985, p. 213.

[2] Harada, T., Taguchi, M., Iwasa, K., and Kai, M., *Digest of Technical Papers of the 1985 SID Symposium*, Playa del Rey, May 1985, p.131.

[3] Maltese, P., *Conf. Record of the 1991 Intl. Display Research Conf.*, San Diego, Oct. 1991, p. 77; also work presented in FLC91, O-34, Boulder, June 1991.

[4] Maltese, P., Piccolo, R., Ferrara V., 1993, *Liq. Crystals*, **15**, 819.

[5] Maltese, P., Dijon, J., Leroux, T. and Sarrasin, D., 1988, *Ferroelectrics*, **85**, 265.

[6] Maltese, P., Dijon, J. and Leroux, T., *Conf. Record of the 1988 Intl. Display Research Conf.*, San Diego, Oct. 1988, p. 98.

[7] Saunders, F. C., Hughes, J. R., Pedlingham, H. A. and Towler, M. J., 1989, *Liq. Crystals*, **6**, 341.

[8] Rieker, T. P., Clark, N. A., Smith, G. S., Parmar, D. S., Sirota, E. B. and Safinya, C. R., 1987, *Phys. Rev. Lett.*, **59**, 2658.

[9] Matuszczyk, T., Maltese, P. and Bernardini, F., presented to the 1st SICL Conf., Amalfi, June 1994, submitted to *Mol. Cryst. and Liq. Crystals.*

[10] Surguy, P. W. H., Ayliffe, P. J., Birch, M. J., Bone, M. F., Coulson, I., Crossland, W. A., Hughes, J. R., Ross, P. W., Saunders, F. C. and Towler, M. J., 1991, *Ferroelectrics*, **122**, 63.

[11] Maltese, P, 1992, *Mol. Cryst. and Liq. Crystals*, **215**, 57.

[12] Shimizu K., Tanaka, Y., Sekikawa, K., Inoue, K. and Hori, H., 1987, *Proc. of the SID*, **28**, 211.

[13] Bowry C., Mosley, A., Nicholas, B. M., *Conf. Record of the 1987 Intl. Display Research Conf.*, London, Oct. 1987, p. 152.

[14] Escher, C., Illian, G., Kaltbeitzel, A., Manero, J., Ohlendorf, D., Rieger, H., Reusch, N., Schlosser, H., Wegener, P. and Wingen, R., *SPIE IS&T Symposium*, San Jose, Feb. 1992.

[15] Maltese, P. and Piccolo, R., *Digest of Technical Papers of the 1993 SID Symposium*, Seattle, May 1993, p. 642.

[16] Hughes, J. R. and Raynes, E. P., 1993, *Liq. Crystals*, **13**, 597, errata corrige, **15**, 281.

[17] Maltese, P., *Conf. Record of the 1993 Intl. Display Research Conf.*, Strasbourg, Aug. 1993, p. 371.

[18] McDonnel, D. G., Bannister, R. W., Graham, A., Hughes, J. R., Pedlingham, H. A. Scattergood, D. C. and Smith, C. J. T., *Digest of Technical Papers of the 1993 SID Symposium*, Seattle, May 1993, p. 654.

[19] Maltese, P., Ferrara, V. and Piccolo, R., *Digest of Technical Papers of the 1994 SID Symposium*, San Jose, June 1994, p. 151.